Motion correction of diffusion-weighted imaging of the liver: use of velocity-compensated diffusion gradients combined with tetrahedral gradients

Masanori Ozaki[1,2], Yusuke Inoue[3], Tosiaki Miyati[2], Hirofumi Hata[4], Shinya Mizukami[5], Shotaro Komi[4], Keiji Matsunaga[3], Reiko Woodhams[3], and Shinichi Kan[3]

[1]*School of Allied Health Sciences, Kitasato University, Sagamihara, Kanagawa, Japan,* [2]*Graduate School of Medical Science, Kanazawa University, Kanazawa, Ishikawa, Japan,* [3]*Department of Diagnostic Radiology, Kitasato University School of Medicine, Sagamihara, Kanagawa, Japan,* [4]*Department of Radiology, Kitasato University Hospital, Kanagawa, Japan,* [5]*Department of Radiology, Kitasato University Hospital, Sagamihara, Kanagawa, Japan*

Introduction:

Diffusion-weighted magnetic-resonance imaging (DWI) with an apparent diffusion coefficient (ADC) is a useful MRI technique for the detection and characterization of liver lesions. A conventional pulse sequence for DWI adds bipolar gradients in three orthogonal directions, after excitation and before readout. These pulsed gradients will induce a phase shift due to cardiac motion as well as cause attenuation of the echo signal due to diffusion of the spins. Therefore, artificial elevation of ADC of the liver occurs due to this effect, which can be reduced by using a velocity-compensated (VC)-DWI as shown in recent studies [1-3]. VC diffusion gradients remove all phase sensitivity to constant-velocity patient motion during the diffusion-weighting period (Fig. 1). However one disadvantage of a VC-DWI sequence is that, for a given b-value, the duration of the VC diffusion gradient pulses must be approximately 1.59 times longer than the Stejskal-Tanner diffusion gradient pulses, which leads to a reduction in the signal-to-noise ratio (SNR). In contrast, the use of diffusion gradient pulses with simultaneous application of all three orthogonal gradients, instead of separate application of the orthogonal gradients, can shorten the duration of the diffusion gradient pulses without reducing b-values. This method can generate four different gradient vectors (Fig. 2), which are called tetrahedral gradients [4-5]. These can be used to obtain isotropic DWI and a higher SNR than with orthogonal gradients. In the present study, we compared a velocity-compensated DWI (VC-DWI) sequence and a VC-DWI sequence combined with tetrahedral gradients (t-VC-DWI) to conventional DWI (c-DWI) in the assessment of ADC of the liver.

Materials and Methods:

All examinations were performed on a clinical MR scanner (Signa HDxt optima edition 1.5T, GE Healthcare, Milwaukee, WI). The system provides a maximum gradient strength of 33 mT/m with a peak slew rate of 120 mT/m/msec. The coil used here was a 12-element body phased array coil. The sequence parameters of single-shot SE-EPI were as follows; TR of 4 or 5 R-R (with respiratory triggering), TE of 76.3 ms (c-DWI), 121.6 ms (VC-DWI), and 95.5 ms (t-VC-DWI), slice thickness/slice gap of 10/0 mm, number of slices of 15, b-values of 0 and 1000 s/mm^2, FOV of 400 mm, matrix of 128, NSA of 4 (orthogonal gradients), 3 (tetrahedral gradients), and spectral spatial radio-frequency fat suppression. In twelve healthy volunteers, the liver was scanned with c-DWI, VC-DWI, and t-VC-DWI sequences. The SNR and ADC were measured over images obtained from each pulse sequence. The SNR was calculated from the signal intensity and the noise was extracted from a single square ROI (7×7 pixels). The ROIs were set in the anterior, medial-lateral, and posterior regions of the right hepatic lobe. ADCs of the right and left hepatic lobes were defined as the averages of the ADCs extracted from three circular ROIs (49 pixels) set in the right and left hepatic lobes. ADC and SNR were compared using parametric tests.

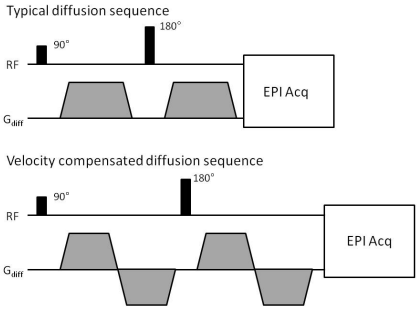

Fig. 1: Typical diffusion sequence (upper) and velocity-compensated diffusion sequence (lower).

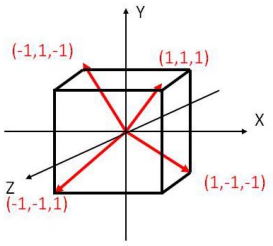

Fig. 2: Spatial configuration of tetrahedral gradient vectors.

Results:

The SNR was significantly higher for t-VC-DWI than for VC-DWI ($P < 0.05$). Figure 3 shows the results of ADC measurement using each pulse sequence. The ADCs of both hepatic lobes were significantly lower for t-VC-DWI than for c-DWI ($P < 0.01$) and for VC-DWI ($P < 0.05$). The ADCs of the left hepatic lobe were significantly lower for VC-DWI than for c-DWI ($P < 0.01$). Table 1 shows the results of comparisons between the ADCs of the right and left hepatic lobes. Although the ADC of the left hepatic lobe was significantly higher than that of the right hepatic lobe for c-DWI ($P < 0.01$), no significant differences in ADCs were found between the right and left hepatic lobes for VC-DWI and t-VC-DWI. Figure 4 shows axial DWIs and ADC maps. Severe signal loss and high ADCs are noted in the left hepatic lobe and the medial portion of the right hepatic lobe for c-DWI.

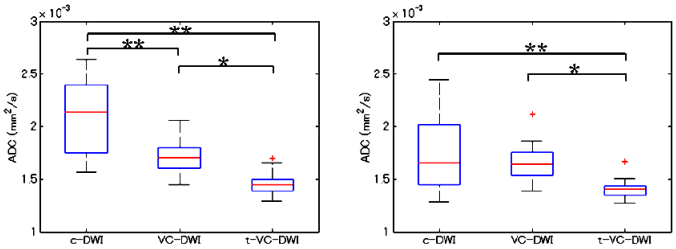

Fig. 3: ADCs using each pulse sequence. Left panel, ADC in the left hepatic lobe; right panel, ADC in the right hepatic lobe; * P<0.05; ** P<0.01.

Table 1 Comparison of ADCs (×10^{-3} mm^2/s) between the right and left hepatic lobes

	Right hepatic lobe	Left hepatic lobe	P value
c-DWI	1.75±0.38	2.10±0.37	0.006
VC-DWI	1.66±0.20	1.72±0.17	0.359
t-VC-DWI	1.41±0.11	1.46±0.12	0.101

Discussion:

Artificial elevation of the ADC of the liver occurs due to cardiac motion [6-7]. Our results suggest that a t-VC-DWI sequence can compensate for the signal loss and artificial elevation of the ADC. The SNR of t-VC-DWI was also improved when compared with VC-DWI. The t-VC-DWI sequence has the capacity to provide imaged with higher b-values (e.g., 1000s/mm^2 or higher) in practical use.

In conclusion, the t-VC-DWI sequence makes it possible to correct of artificial elevation of the ADC of the liver due to cardiac motion, with preserved SNR.

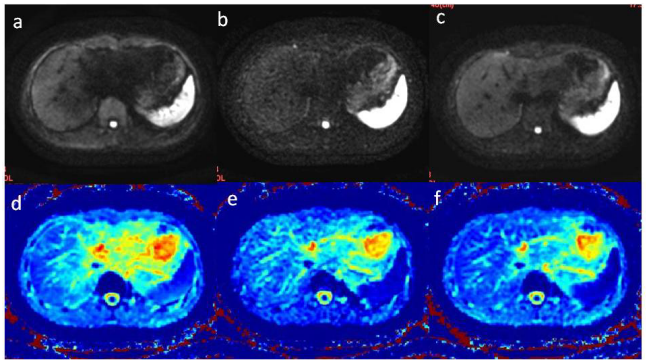

Fig. 4: DWIs (a-c), and ADC maps (d-f) acquired with c-DWI (a, d), VC-DWI (b, e), and t-VC-DWI (c, f).

Reference:

1. Johnson GA, Maki JH, *Invest Radiol*. **26(6)**:540-5 (1991)
2. Winter J.D et al, *Proc ISMRM* **2129** (2003)
3. Ogino T et al, *Proc ISMRM* **4068** (2009)
4. Conturo TE, et al. *Magn. Reson. Med.* **5**:399-412 (1996)
5. Hori M et al, *Proc ISMRM* **845** (2006)
6. Nasu K et al, *MAGMA* **20**:205-211 (2007)
7. Thomas C et al, *MAGMA* **22**:319-325 (2009)